https://doi.org/10.15407/scine20.03.067

LINEVYCH, Ya. O.[1] (https://orcid.org/0000-0002-8399-034),
KOVAL, V. M.[1] (https://orcid.org/ 0000-0002-3898-9163),
DUSHEIKO, M. H.[1] (https://orcid.org/ 0000-0003-3476-4220),
and LAKYDA, M. O.[2] (https://orcid.org/0000-00019973-9849)

[1] National Technical University of Ukraine “Igor Sikorsky Kyiv Polytechnic Institute”,
37, Peremohy Ave., Kyiv, 03056, Ukraine,
+380 44 204 9074, fel@kpi.ua
[2] National University of Life and Environmental Sciences of Ukraine,
15, Heroiv Oborony St., Kyiv, 03041, Ukraine,
+380 44 527 8205, rectorat@nubip.edu.uav

HUMIDITY DIODE SENSORS BASED ON 1D NANOSIZED SILICON STRUCTURES

Introduction. *Humidity measurement is essential in microelectronics, aerospace, biomedical, and food industries, as well as in households for climate control. Currently, various types of devices have been used as humidity sensors: capacitive, resistive, diode, gravimetric, optical structures, field-effect transistors and devices based on surface acoustic waves.*

Problem Statement. *Today, there is a need to develop IC-compatible humidity sensors that have high sensitivity and low cost. To this end, silicon nanowires have been successfully used in resistive and capacitive humidity sensors. However, there is a lack of research on the nanowire effect on device parameters of diode-type humidity sensors.*

Purpose. *To develop diode sensors based on silicon nanowires and to determine the effect of process parameters of synthesis and structural features of nanowires on the performance of humidity sensors.*

Materials and Methods. *The process of sensor fabrication includes several steps: chemical cleaning of silicon wafer, synthesis of silicon nanowires using standard or modified metal-assisted chemical etching, phosphorus diffusion to create a p-n junction, front and back metallization. The surface morphology of the nanostructures has been studied by scanning electron microscopy. The humidity-sensitive characteristics have been studied with the use of salt hygrostats.*

Results. *It has been shown that the addition of one-dimensional silicon nanostructures to the diode-type sensor significantly improves its characteristics. The rectification ratio increases from 161 to 1807, the response ups from 4.5 to 25, the sensitivity grows from 1.6 to 4.02 (%RH)−1, while the response time and recovery time are*

Citation: Linevych, Ya. O., Koval, V. M., Dusheiko, M. H., and Lakyda, M. O. (2024). Humidity Diode Sensors Based on 1D Nanosized Silicon Structures. *Sci. innov.*, 20(3), 67—81. https://doi.org/10.15407/scine20.03.067

reduced from 85/90 to 25/30 s, the hysteresis value goes down from 75 to 16%, the signal deviation after cycling drops from 15 to 3%, and the signal fluctuation during continuous device operation decreases from 17 to 15%.

Conclusions. *The results have shown that the use of a simple and cheap nanowire synthesis technology is effective to produce humidity sensors.*

Keywords: metal-assisted chemical etching, silicon nanowires, 1D nanostructures, silicon diode, and humidity sensors.

Measuring humidity in the environment has become critically important in various areas of human activity: industrial and agricultural production, food storage, aerospace, biomedical, and food industries. It is known that for comfortable living the relative humidity should range within 40—60% [1]. Therefore, humidity sensors are installed in various climate systems. In the food industry, relative humidity for food storage should be 85—90%. However, in microelectronics, humidity should be minimal (less than 1%) [2] to avoid negative impact on the chip manufacturing process. In addition, humidity is a key factor in early warning of forest fires, as it directly depends on the evaporation of water from combustibles. Generally, the fire risk is high at a relative humidity (RH) below 55%. Catastrophic fires may occur when RH is below 30% [3]. Humidity is also an important health indicator in the medical field. For example, respiratory humidity decreases significantly when the human body is dehydrated, or respiratory failure is accompanied by a rapid increase in respiratory rate [4].

Currently, various types of devices are used as humidity sensors: capacitive [5], resistive [6], diode [7], gravimetric [8], and optical structures [9], as well as field-effect transistors [10] and devices based on surface acoustic waves [11]. Some of these devices are quite bulky and not compatible with integrated technology (gravimetric and optical devices, as well as sensors based on surface acoustic waves). Today, there is a need to develop integrated microsensors as part of a smart sensor platform that can be installed indoors or attached to human items (mobile phones, glasses, etc.). With this in mind, diode, capacitive, resistive sensors are the most suitable for such applications, as they are manufactured with the use of standard group microelectronic technology that provides micro-sized and low-cost devices. However, the resistive sensors have a slow response, while the capacitive sensors require a more complex measurement scheme. Therefore, the diode type of humidity sensors is the most attractive for these applications.

In the last decade, there has been a growing interest in the use of various types of nanomaterials to miniaturize the sensors and to increase their sensitivity. Various types of nanostructures, including 1D structures, have been successfully used for this purpose. Nanowires are one-dimensional nanostructures in the form of continuous wires or fibers that have a nanoscale width (diameter) and a length that is much larger than the width. Nanopores are nano-sized holes in a material, the longitudinal size of which usually reaches several micrometers. The array of nanoholes is an inverted structure in relation to the array of nanowires. This ensures a high aspect ratio [12]. 1D structures are very promising because they have a number of advantages for sensor applications:

1) large surface-to-volume ratio that allows more atoms to participate in surface reactions, which increases sensing surface area of a sensor;

2) increased diffusion rate of electrons and holes towards side surface of device may facilitate rapid desorption of analyte molecules from device surface, i.e., the reaction speed of such sensors increases.

Today, various materials have been used in sensors to make nanowires/nanofibers: In_2O_3 nanofibers [13], TiO_2 nanofibers [14], ZnO nanofibers [15], CuO nanofibers [16], cellulose nanofibers [17], Ag@TiO_2 nanofibers [18], WO_3 nanofibers [19], and silicon nanowires (SiNWs) [20]. Among them, the most notable is silicon material, as it has

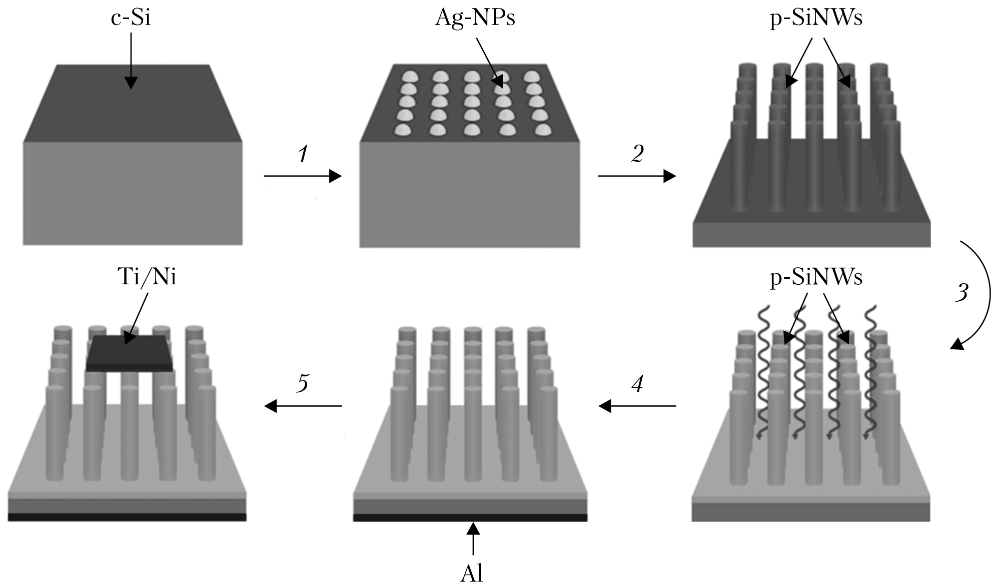

Fig. 1. Schematic representation of the manufacturing process of humidity sensors based on SiNWs: *1* — deposition of Ag-NPs (first stage of MACE); *2* — etching of silicon (second stage of MACE); *3* — formation of *p-n* junction (phosphorus diffusion); *4* — deposition of back contact and annealing (HF magnetron sputtering of Al); *5* — formation of a two-layer frontal contact (electron-beam evaporation of Ti and Ni through a mask with rectangular holes)

significant advantages for the manufacture of 1D nanostructures: low material cost, well-developed processing technology, non-toxicity, and compatibility with integrated circuits. In addition, humidity sensors based on silicon nanowires have a high sensitivity due to the fact that their surface is covered with a significant number of Si-OH groups, which provides it significant hydrophilicity.

Silicon nanowires can be synthesized by one of the two general approaches: the bottom-up approach and the top-down approach. The bottom-up approach involves the growth of silicon nanowires from individual atoms with the following techniques: chemical vapor deposition (CVD) [21] and vapor-liquid-solid growth (VLS growth) [22]. The advantages of this approach include the high orderliness of SiNWs, but the disadvantages are the relative complexity of the process and the low density of synthesized SiNWs. In the top-down approach, the clusters of a single crystal substrate are removed. This results in the formation of one-dimensional columns (nanowires): Lithography and Etching [23] and Metal Assisted Chemical Etching (MACE) [24]. The advantages of this approach, in particular the method of MACE, include high density and smooth walls of the resulting array of silicon nanowires, as well as relative simplicity and low cost. To date, successful attempts have been made to use silicon nanowires in the resistive [25] and the capacitive type of humidity sensors [26]. However, there is a lack of research on the diode-type humidity sensors based on SiNWs, which is the focus of this paper.

The purpose of this research is to develop the diode humidity sensors based on silicon nanowires and to determine the effect of technological parameters of SiNWs synthesis on device performance.

The production technology of humidity sensors consists of the following steps (Fig. 1): chemical cleaning of silicon wafers; metal-assisted chemical etching to synthesize silicon nanowires on the surface of silicon wafers; diffusion operation to create a *p-n* junction in the nanowires; front and back metallization.

There have been used boron-doped c-Si substrates of different resistivity (1 and 10 Ω·cm), which were subjected to a three-stage cleaning process. During the first stage, mechanical and organic contaminants are removed in a peroxide-ammonia solution of $NH_4OH/H_2O_2/H_2O$ (1 : 1 : 3) at 80 °C for 10 min. During the second stage, the residual metal ions are removed in a peroxide-chlorine solution $HCl/H_2O_2/H_2O$ (1 : 1 : 3) at 80 °C for 10 min. In the third stage, the wafers are immersed in a hydrofluoric acid solution H_2O/HF (100 : 0.5) for 30 s to remove surface silicon oxide. After each step, the wafers are rinsed in a three-stage bath of deionized water (60 °C /40 °C/20 °C) for 20 min and then dried in a centrifuge.

To synthesize silicon nanowires, we have used a two-step method of metal-assisted chemical etching. The standard approach for the MACE operation includes the two stages: deposition of silver nanoparticles (Ag NPs) on the surface of silicon wafer and etching of it under these nanoparticles.

The solution for the first stage of MACE is prepared on the basis of silver nitrate nanopowder: 68 mg of $AgNO_3$ is dissolved in 4.42 ml of 40% HF solution and 10 ml of H_2O. Then H_2O is added to the mixture to obtain 20 ml solution. The duration of the first stage of MACE ranges from 10 to 60 s. The solution for the second stage of MACE is prepared on the basis of hydrogen peroxide: 11 ml of 40% HF, 30 ml of H_2O, and 0.8 or 0.4 ml. The duration of the second stage of MACE ranges from 30 to 90 min. The obtained nanowires are approximately 5 μm in height [20].

Also, additional technological operations are used to modify the structural parameters of silicon nanowires: silicon wafer texturing and processing in isotropic/anisotropic etchants. The texturing operation is performed before the MACE process on a separate group of samples in order to obtain a more developed humidity-sensitive surface due to the presence of texture pyramids. The samples are textured in solution: 970 ml of H_2O, 30 g of KOH, 70 ml of IPA, for 15 min at 75 °C. The treatment in isotropic/anisotropic etching agents is carried out after the MACE process in order to remove porous (broken) layers on the surface of nanowires. Two types of etching agents are used for the experiment: an acidic etchant of $HF/HNO_3/CH_3COOH$ (1 : 4 : 4), for isotropic etching of the surface, and an alkaline etchant of $NaOH/IPA/H_2O$ (2 : 10 : 88), for anisotropic etching.

The next stage after the SiNWs synthesis is the formation of a *p-n* junction. For this purpose, phosphorus dopant is introduced in silicon nanowires in a diffusion furnace. Firstly, p impurities are introduced into the surface layer of silicon at a temperature of 750 °C for 5 min. After that, the P impurities penetrate at a temperature of 830 °C for 20 min. As a result, an n-type silicon layer with a specific surface resistivity of 50 Ohm/ϒ is obtained. The depth of the diffusion layer is near 0.1 μm. Given the length of obtained nanowires, inside them there is formed a *p-n* junction.

Next, a continuous Al back contact is deposited on the samples by the RF magnetron sputtering technique. The operating parameters in the vacuum chamber during deposition are as follows: the voltage is 400 kV, the current is 4 A, argon pressure is $3 \cdot 10^{-7}$ mmHg, and the deposition time is 40 min. The aluminum film is then annealed in a diffusion furnace at 650 °C under a nitrogen atmosphere. As a result of the operation, a 1.5 μm thick back contact is obtained.

The process of device manufacturing is completed by forming of dot-type frontal contacts. The electron beam deposition technique has been used to obtain of Ti/Ni metal contacts. Ti and Ni films are deposited in a vacuum chamber under the following parameters: the chamber pressure is 10^{-5} mmHg, the voltage is 13 kV, and the current is 120 mA. The deposition time for titanium and nickel is 3 and 20 min, respectively. As a result, there are formed frontal contacts with a thickness of about 0.5 μm.

The surface morphology of humidity sensors based on SiNWs has been investigated by a scanning electron microscope (SEM) REM-106U in the secondary electron mode. The current-voltage characteristics of the devices are measured by means of Power Supply HM8143 and a digital

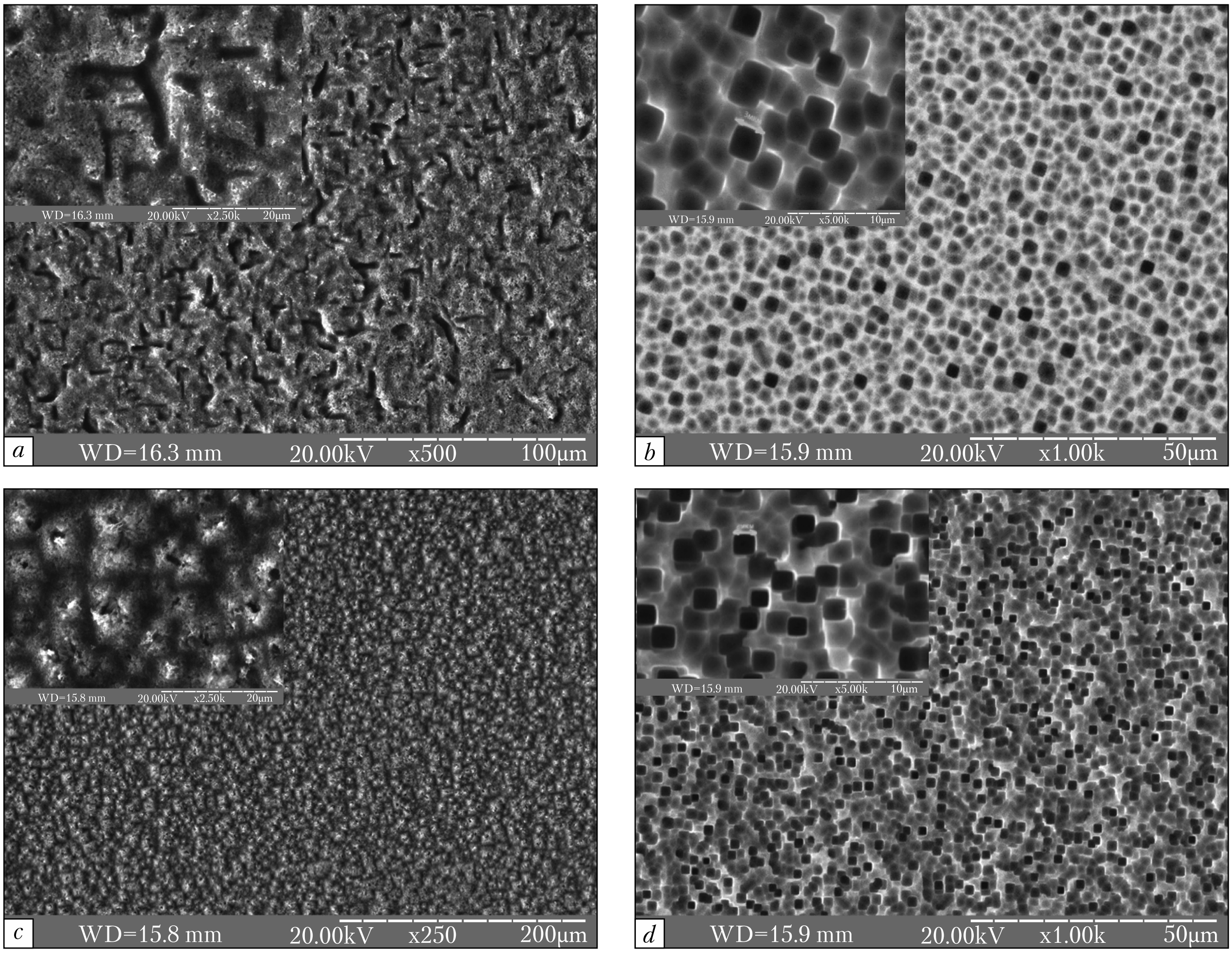

Fig. 2. SEM images of non-textured (*a, b*) and textured (*c, d*) MACE Si surface without (*a, c*) and with (*b, d*) treatment in acid etchant

voltmeter-amperemeter MS8040. The humidity-sensitive characteristics of the sensors are measured by hygrostats based on saturated salt solutions, which generate different levels of relative humidity: LiCl — 12%, $MgCl_2$ — 33%, NaBr — 60%, NaCl — 75%, KCl — 85%, and H_2O — 98%. The humidity in hygrostats is controlled by thermo-hygrometer EZODO HT-390. The humidity-sensitive characteristics (graphs) of the obtained sensors are measured several times until thermodynamic equilibrium is established in salt hygrostats. Below, the equilibrium curves are presented.

Surface morphology of SiNWs. From the SEM image in Fig. 2, *a*, we see the formation of groove-like holes (or nanowire walls) on a polished silicon wafer after MACE process. The lateral length of the grooves that are distributed evenly over the surface ranges from 2 to 10 μm. Figure 2, *c* shows that the textured silicon wafer is characterized by pyramidal structures that evenly cover its surface. It should be noted, silicon surface after MACE looks somewhat diffuse and blurred, which is explained by the presence of surface disturbed layers and natural oxide (insets in Fig. 2, *c, d*). The disturbed layers as surface defects can capture electrical charge carriers during current flow [27]. To remove these layers, we have used acid (isotropic) and alkaline (anisotropic) subsequent et-

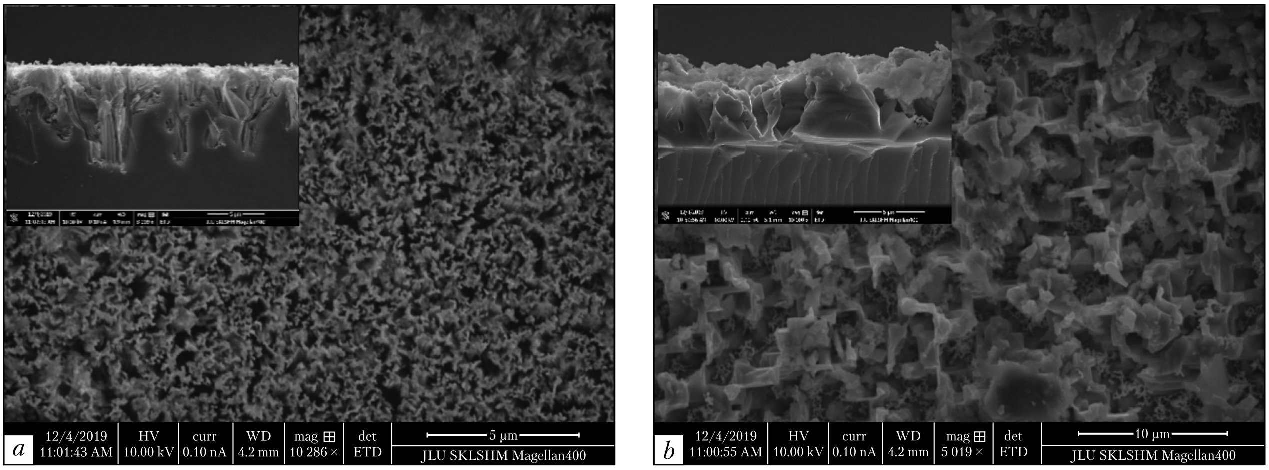

Fig. 3. 2D SEM images of non-textured MACE Si surface without (*a*) and with (*b*) treatment in alkaline etchant (corresponding 3D images in the insets)

ching. From the SEM images (Fig. 2, *b, d*), we have concluded that the acid etchant removes the rough surface layer, which results in a smoother surface and well-defined nanostructures (nanoholes). It is obviously, nanoholes appear on the surface due to etching in depth at the same speed of different crystallographic faces of a single crystal. The obtained holes are square in shape with a side size of about 3 μm and cover the entire surface of the sample (Fig. 2, *b*). The depth of the nanoholes is obviously different: the black nanoholes are deeper than the gray ones. Figure 2, *d* shows that the treatment of a textured Si surface in an acid etchant results in an identical morphology. However, the size of obtained nanoholes is somewhat smaller, as the length of the square side is about 2 μm. A characteristic feature of the textured samples is that the number of deep holes is much larger than that of those on a polished surface.

Figure 3 shows 2D and 3D SEM images (in insets) of a Si surface after MACE process without and with additional alkaline treatment of polished substrates. Figure 3 features that the nanowire walls are separated by grooves, but with disturbed defective layer. After the treatment in an alkaline etchant, the width of the grooves increases. Unlike the isotropic etching, the anisotropic one depends on crystallographic orientation. This means that the etching process is carried out along certain crystallographic directions. As a result, it is possible to observe mostly lateral chemical etching of the groove-like holes rather than deep etching into the substrate as in the case of an isotropic etchant.

Electrical properties of SiNWs diodes. The electrical properties of SiNWs-based diode-type humidity sensors have been studied by means of the dark current-voltage curves (I—V curves) shown in Fig. 4, *a*). The obtained sensors are characterized by rectifying properties (Fig. 4, *a*). The rectification ratio is calculated as the ratio of forward current to reverse current at a voltage of 1 V. The maximum rectification ratio obtained in this research is 1837.

The influence of the SiNW fabrication parameters on the electrical parameters of *p-n* junction has been determined. In particular, the increasing duration of the first and second MACE stages that are responsible for the geometry of silicon nanowire array has a significant effect on the device parameters. Thus, with an increase in the deposition time of silver nanoparticles from 10 to 60 s, the rectification ratio increases significantly (from 62 to 439). This may be due to an increase in the density of deposited metal nanoparticles on the silicon surface, which results in the forma-

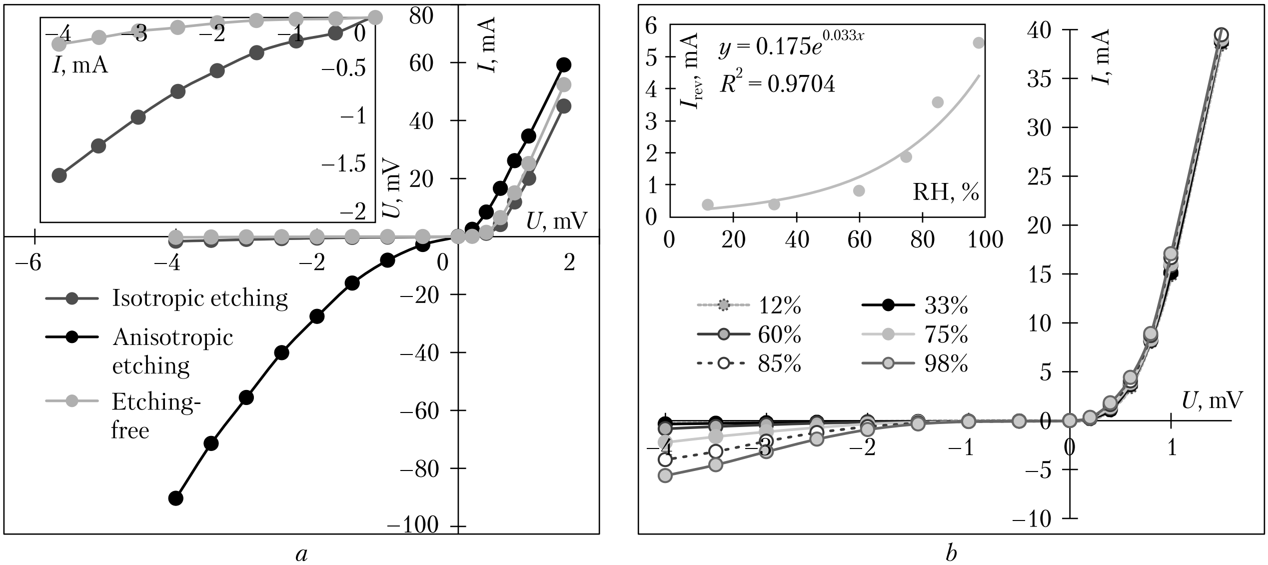

Fig. 4. The influence of additional etchants (*a*) and relative humidity (*b*) on I—V characteristics of humidity sensors based on SiNWs (in the insets: the reverse currents without and with treatment in isotropic etchant (*a*) and the effect of RH on the reverse current at 4 V (*b*))

tion of well-developed surface [12]. As a result, the device direct currents and the rectification ratio increase. The change of etching time during the second MACE stage in the range from 30 to 150 min causes a 6-fold decrease in the rectification ratio. Obviously, prolonged etching process reduces reverse currents through *p-n* junction, thereby increasing the rectification ratio.

Also, we have studied the effect of etching agent content at both MACE stages. It has been found that a lower content of $AgNO_3$ (34 mg) leads to a 20-fold increase in the rectification ratio (from 17 to 332). This can be explained by the fact that with a reduced amount of metal nitrate, no silver dendrites are formed, as it has been confirmed by our previous results [12]. A change in the hydrogen peroxide content from 0.8 to 0.4 ml has resulted in a slight increase in the rectification ratio from 332 to 392. This may be due to the fact that a lower concentration of H_2O_2 in the solution causes a more uniform etching of silicon surface because of the release of fewer hydrogen bubbles that interfere the uniform etching.

The reesistivity of the initial silicon wafer has a significant impact on the rectifying properties of diode structures with nanowires. The use of Si substrate of 10 Ω · cm significantly increases the rectification of such structures (from 252 to 925). The point is that a decrease in the concentration of charge carriers leads to a decrease in the reverse current, which in turn increases the rectification ratio.

Surface texturing causes a decrease in the rectification ratio by an order of magnitude (from 840 to 84), because of a significant increase in the reverse current. Also processing of Si MACE substrate in an additional etchant leads to a decrease in the rectification ratio, both in the case of an isotropic etchant (by a factor of 2), and in the case of an anisotropic etchant (by a factor of 100). A significant deterioration in the rectifying properties after alkaline etchant has beeen shown because of surface heterogeneity that makes impossible the formation of a high-quality *p-n* junction.

To compare the device characteristics, a diode sensor without nanowires has been made. Such sensor has a rectification ratio of 161. It is more than an order of magnitude worse than the maxi-

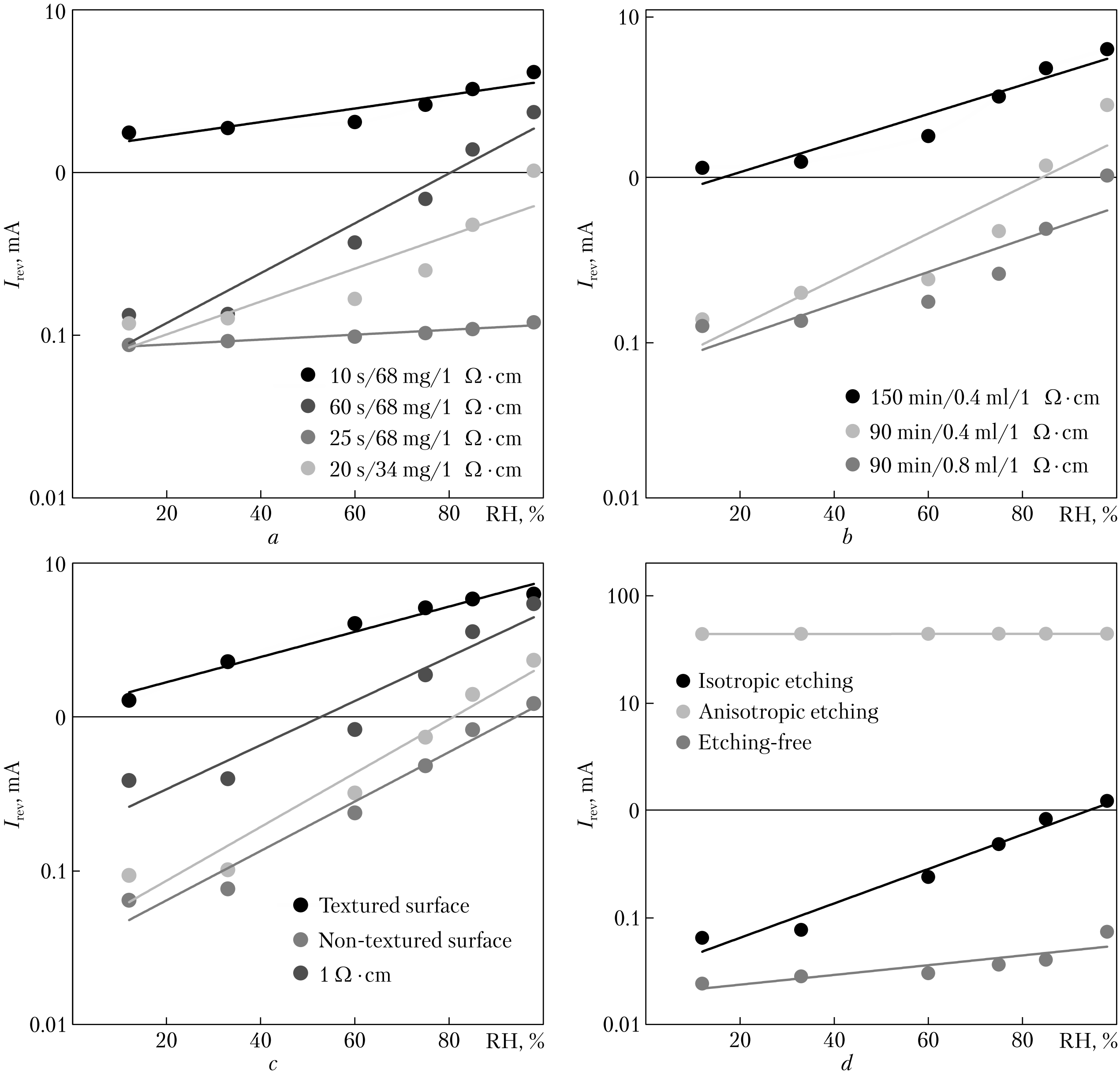

Fig. 5. The influence of parameters of the first stage of MACE (*a*), parameters of the second stage of MACE (*b*), resistivity of the substrate and texturing (*c*), processing in additional etchants (*d*) on the response curves of humidity sensors based on SiNWs

mum coefficient for the diode sensors with nanostructures (1837). It should also be noted that, depending on the morphology of obtained nanostructures, their presence in the sensor structure can improve or worsen its electrical properties. The following technological parameters of SiNWs synthesis, which contribute to the improvement of the rectifying properties of SiNWs structures, as compared with the planar *p-n* junction, can be distinguished: the deposition time should exceed 10 s, the etching time should be less than 150 min, the resistivity of silicon substrate is 10 Ω · cm, no additional etching agents or surface texturing should be involved.

Humidity-sensing properties of SiNWs diodes. Response and sensitivity. The principle of operation of the diode-type humidity sensor is to change the reverse current depending on the level of relative humidity. Figure 4, *b* shows that a change in the relative humidity from 12% to 98% has almost no effect on the direct current, while the reverse current undergoes noticeable changes. The maximum sensitivity has been demonstrated at a reverse voltage of 4 V, which is chosen as the operating point of the device.

As the level of RH increases, so does the reverse current of the sensors (Fig. 4, *b*). This dependence can be approximated by an exponential function. The response of diode humidity sensor is defined as change in the reverse current during measurement within a given humidity range. The sensitivity of humidity sensor is defined as the exponent of approximating curve. Depending on the technological parameters of MACE, the sensor response varies from 1 to 25 times, while the sensitivity ranges from 0.01 to 4.02 $(\%RH)^{-1}$.

In this research, we have determined the effect of the parameters of the first MACE stage (the Ag nanoparticle deposition time and the $AgNO_3$ content) on the response of humidity sensors (Fig. 5, *a*). It has been found that an increase in the deposition time of Ag nanoparticles improves the response magnitude and, accordingly, the sensitivity of humidity sensors based on SiNWs. In particular, the response curves (Fig. 5, *a*) show an increase in the response value from 2.7 to 17.7. Reducing the content of $AgNO_3$ by half (from 68 to 34 mg) in the solution improves the response value from 1.4 to 8.7. This is because a smaller amount of metal nitrate reduces the possibility of silver dendrite formation.

Also, we have studied the influence of the parameters of the second MACE stage (the etching time and the H_2O_2 content) on the response of humidity sensors (Fig. 5, *b*). It has been shown that increasing the etching time from 30 to 150 min worsens the response of SiNW-based humidity sensors, and namely: a decrease in the response ranges from 25 to 5.5 times. The almost 5-time decrease in the response is caused by the fact that with a longer etching time, the reverse currents through *p-n* junction significantly increase, thereby reducing the device response. While varying the hydrogen peroxide content from 0.8 to 0.4 ml, we have observed an increase in the response from 8.7 to 21.7 times. The significant improvement in the response value with a decrease in H_2O_2 content may be caused by the fact that fewer hydrogen bubbles are released during the etching process, which ensures uniform etching.

The influence of the initial substrate on the humidity sensitivity has been determined: a change in the resistivity from 1 to 10 $\Omega \cdot$ cm leads to an increase in the response from 14.1 to 25 times (Fig. 5, *c*). The textured surface before the MACE process leads to a significant deterioration (almost 4 times) in the response. This is obviously because of disturbed layers that result in a significant increase in the magnitude of reverse current.

The treatment with an additional isotropic etchant significantly improves the device sensitivity: the response value increases from 2.4 to 19 times (Fig. 5, *c*). The use of an anisotropic etchant, on contrary, worsens the humidity-sensitive characteristics: the response decreases from 2.4 to 0.99 times. This is due to the fact that the acidic etchant removes disturbed layers and structural defects, which increases the lifetime of minor charge carriers. In turn, the alkaline etchant results in a structurally heterogeneous surface on which it is impossible to form a high-quality *p-n* junction.

For comparison, the response of diode humidity sensors without nanowires is 4.5 times. It is significantly worse than the maximum value for the devices with nanostructures (25 times). However, it should be noted that, depending on the morphology of the obtained nanostructures, their presence in the device structure can worsen its humidity-sensitive characteristics. Therefore, we can distinguish the following technological parameters of SiNWs synthesis, which improve the response of diode structures: the deposition time of Ag

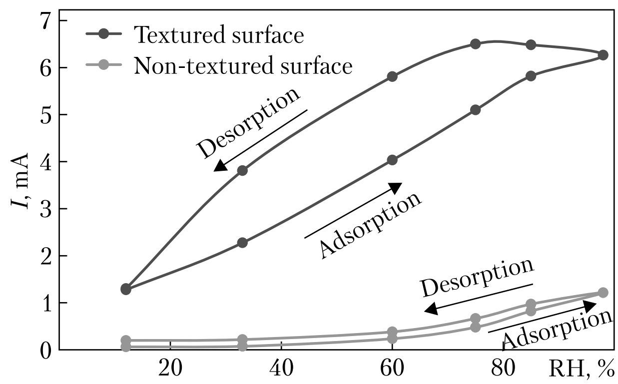

Fig. 6. The effect of surface texturing on the hysteresis loop of humidity sensor based on SiNWs

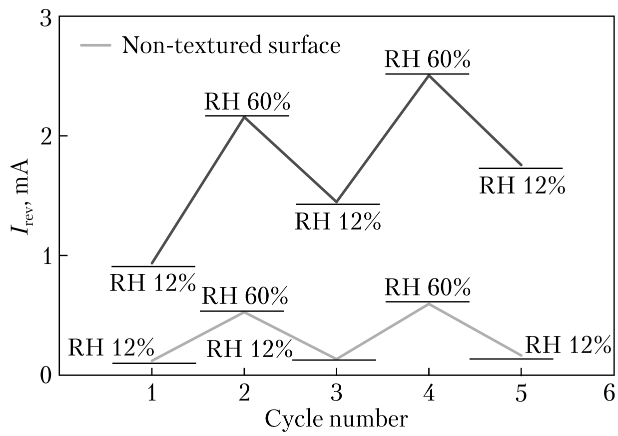

Fig. 7. The effect of texturing on signal deviation during cycling measurements of humidity sensors based on SiNWs

nanoparticles should exceed 20 s, the etching duration should be less than 150 min, the treatment in an isotropic etchant should be applied. In turn, the texturing and use of alkaline etching result in a significant degradation of the device response.

In order to compare the sensitivity of obtained sensors with other types of sensors based on silicon nanowires (capacitive and resistive), it is necessary to calculate this parameter in relative units (the relative change of measured device parameter (current, capacitance or resistance) divided by the range of relative humidity). Hence, the sensitivity for the obtained sensors is 24.5% / (%RH), while that of the capacitive sensor is 4.8% / (%RH) [28] and that of the resistive sensor is 3.01% / (%RH) [29]. So, the sensor developed in this research is more sensitive by an order of magnitude than the existing analogs.

Reversibility. The hysteresis curve is taken with a gradual increase and gradual decrease in the humidity in the range of RH from 12 to 98% (Fig. 6). The reversibility of humidity diode sensor has been determined by comparing the maximum difference in the values of reverse current (ΔI_{max}) during adsorption and desorption to the maximum reverse current drop ($I_{max} - I_{min}$) over the entire measurement RH range:

$$\gamma H = \pm \frac{(\Delta I_{max})}{(I_{max} - I_{min})}.$$

Depending on the technological parameters of MACE, the minimum value of the device hysteresis is 16.1%. The influence of technological parameters on the reversibility of sensors has been determined. Thus, with an increase in the time of deposition of Ag nanoparticles from 10 to 60 s, the hysteresis value decreases from 50 to 34.3%. An increase in the etching time in the range from 30 to 90 min causes an increase in the hysteresis value from 39.5 to 45.4%. Also, the influence of the content of etching agents at both MACE stages has been studied. It has been shown that a lower content of $AgNO_3$ (34 mg) leads to a deterioration in the device reversibility (the hysteresis increases from 18.2 to 63.8%). While varying the H_2O_2 content from 0.8 to 0.4 ml, we have observed a slight decrease in the hysteresis value from 63.8 to 52.9%.

It has also been found that the resistivity of initial silicon wafer has almost no effect on the device reversibility (1 Ω cm — 35.3%, 10 Ω · cm — 39.5%). As one can see from Fig. 6, the presence of surface texturing leads to a more than 2-fold deterioration in the reversibility of humidity sensors. The treatment in an additional etchant results in a 3-fold decrease in the hysteresis value, in the case of isotropic etchant, and in a slight decrease in the hysteresis value from 55.1 to 40.7%, in the case of anisotropic etchant.

ISSN 2409-9066. Sci. innov. 2024. 20 (3)

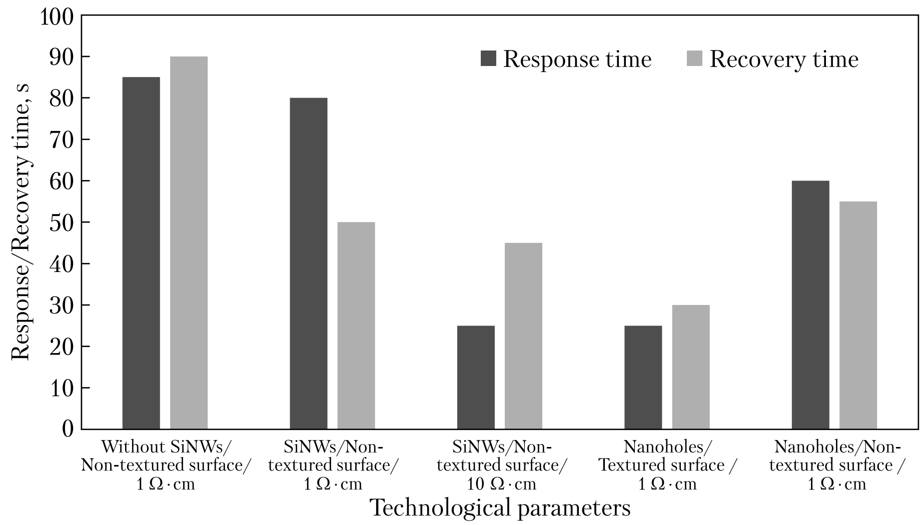

Fig. 8. The influence of technological parameters on the response time and recovery time of humidity sensors based on SiNWs

To compare the reversibility of diode humidity sensors, a sensor without nanowires has been fabricated. Its hysteresis value is 75.2%. It is much worse than the minimum hysteresis value for the diode humidity sensors with nanostructures (16.1%). There may be distinguished the following technological parameters of SiNWs synthesis, which contribute to improving the reversibility of humidity sensors based on SiNWs, as compared with those without them: the deposition time of silver nanoparticles should exceed 20 s, the etching duration should be less than 90 min, the treatment in an isotropic etchant should be applied.

Repeatability. The study of diode sensor repeatability has been based on changes in the sensor signal, as compared with it's initial value, during a cyclic change between two fixed humidity levels: 12% — 60% — 12% — 60% — 12% RH (Fig. 7). It has been found that an increase in the Ag-NPs deposition time to 60 s reduces the amount of signal deviation during cycling measurements from 17 to 3%. Also, it has been determined that for improved repeatability of sensor signal (9%), the etching time and the hydrogen peroxide content should be 90 min and 0.4 ml, respectively. Changing the substrate resistivity from 1 to 10 Ω · cm leads to a decrease in the signal deviation from 17 to 14%. The textured surface results in a deterioration in the device repeatability by 18% (Fig. 7).

The minimum deviation of signal in the sensors with SiNWs is 3%, while in the sensors without them it is equal to 15%. However, depending on the morphology of obtained nanostructures, their presence in device structure may deteriorate the repeatability. The following technological parameters of SiNWs synthesis, which do not cause a deterioration in the value of signal deviation during cycling measurements: the deposition time of Ag nanoparticles should be of 20—60 s, the duration of etching should be 90—30 min, and the hydrogen peroxide content is 0.4—0.8 ml, no texturing or using any additional etchants.

Response time and recovery time. The device response time is measured after moving from an environment with RH of 12% to an environment with RH of 60%. The device recovery time is measured after moving in the opposite direction. The response time is determined at the point when the sensor signal reaches 90% of the steady-state value, while the recovery time is measured at the point when the sensor signal reaches 10% of the steady-state value. As can be seen from Fig. 8, the resistivity of the initial silicon wafer has a significant impact on the response and recovery time of diode structures. The use of Si substrate

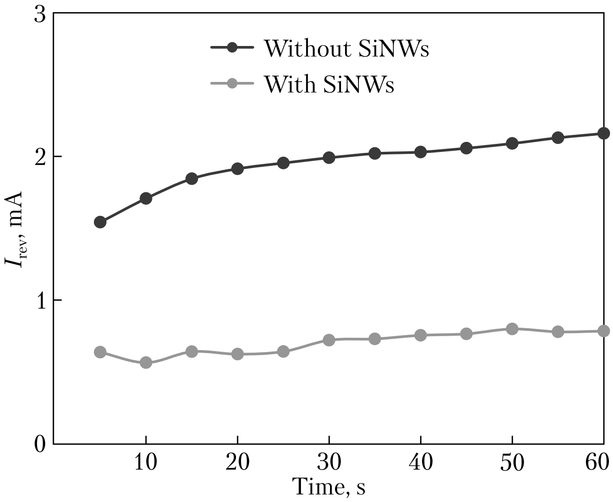

Fig. 9. The effect of SiNWs on the short-term stability of humidity sensors based on SiNWs

with a resistivity of 10 Ω · cm significantly improves the response time (from 80 to 25 s) and slightly reduces the recovery time (by 5 s). The texturing surface also improves the device speed: the response time decreases from 60 to 25 s, and the recovery time is reduced from 55 to 30 s. In general, it has been found that the sensors with SiNWs show lower response/recovery time than the humidity sensors without SiNWs. Thus, the response time for humidity sensors without SiNWs is 85 s, while the recovery time is 90 s. At the same time, the minimum values of these parameters for humidity sensors with SiNWs are 25 and 30 s, respectively (Fig. 8).

The comparison in terms of device speed of the obtained sensors has showed that they are of the same order or better than the existing analogs based on silicon nanowires. So, the response/recovery time of developed device is 25s / 30s, that of the capacitive sensor is 39s / 24s [28], and that of the resistive sensor is 100s / 60s [29].

Short-term stability. The short-term stability of diode sensors is evaluated on the basis of time dependence of reverse current. The measurements are made for 1 hour at two humidity levels of RH (12 and 60%). As can be seen from Fig. 9, in sensors without SiNWs, a thermodynamic equilibrium is established, as a result of worse dynamic characteristics of such structures. In sensors based on SiNWs, there is a deviation of signal within average level due to random fluctuations. The signal fluctuation is defined as deviation from the average level in percent. It has been found that the presence of a textured surface and a substrate with a resistivity of 10 Ω · cm improves the short-term stability of the device by 10—11%. Also, it has been found that the sensors based on SiNWs have somewhat better short-term stability (fluctuation of 15%) than the devices that do not contain them (fluctuation of 17%).

In this research, the diode humidity sensors based on silicon nanowires have been fabricated and the influence of SiNWs synthesis parameters on the structural, electrical, and humidity-sensitive characteristics of the devices has been determined. It has been found that the addition of one-dimensional silicon nanostructures to diode-type humidity sensor significantly improves its electrical and sensitive characteristics: the rectification ratio, from 161 to 1807; the response, from 4.5 to 25; and the sensitivity, from 1.6 to 4.02 $(\%RH)^{-1}$, while the following parameters decrease: the response time and recovery time, from 85/90 to 25/30 s, the hysteresis value, from 75 to 16%, the signal deviation after cycling, from 15 to 3%, and the signal fluctuation during short-term stability test, from 17 to 15%. The direction of changing technological parameters in the standard MACE process to obtain the improved characteristics of humidity sensors are as follows: increasing the Ag-NPs deposition time from 20 to 60 s, decreasing the silicon etching time, from 90 to 30 min; the $AgNO_3$ content, from 68 to 34 mg; and the H_2O_2 content, from 0.8 to 0.4 ml; increasing the resistivity of Si substrate, from 1 to 10 Ohm · cm. The additional treatment before MACE operation (texturing) improves the dynamic characteristics of the sensor (response time/recovery time and short-term stability). The additional treatment after MACE operation in anisotropic etchant results in degrading all sensor parameters, while that in isotropic etchant improves the static characteristics (response and reversibility).

The obtained results have shown that the use of a simple and cheap nanowire synthesis technology is effective to produce humidity sensors. The direction of further research is to improve the sensor stability and to apply breath sensors for analyzing human respiratory activity.

REFERENCES

1. Pan, S., Gayathri, T., Reshma, T., Mang, S. (2022). A sensitive humidity sensor at low pressure with SnO_2. *Sensors and Actuators A: Physical*, 346, 113835. https://doi.org/10.1016/j.sna.2022.113835.
2. Nikulicheva, T. B., Zakhvalinskii, V. S., Pilyuk, E. A., Nikulin, I. S., Vyazmin, V. V., Mishunin, M. V. (2023). New humidity sensor material ($CaSO_4 \cdot 2H_2O$) 0.975-($CuSO_4 \cdot 5H_2O$) 0.025. *Materialia*, 27, 101662. https://doi.org/10.1016/j.mtla.2022.101662.
3. Zheng, F., Li, M., Li, C., Zhou, B., Xuan, X., Li, H. (2022). Wireless surface acoustic wave humidity sensor with chitosan/porous cyclodextrin — TiO_2 composites for monitoring air and human respiration. *Sensors and Actuators B: Chemical*, 379, 133235. https://doi.org/10.1016/j.snb.2022.133235.
4. Fang, H., Lin, J., Hu, Z., Liu, H., Tang, Z., Shi, T., Liao, G. (2020). $Cu(OH)_2$ nanowires/graphene oxide composites based QCM humidity sensor with fast-response for real-time respiration monitoring. *Sensors and Actuators B: Chemical*, 304, 127313. https://doi.org/10.1016/j.snb.2019.127313.
5. Zhao, Y., Yang, B., Liu, J. (2018). Effect of interdigital electrode gap on the performance of SnO_2 — modified MoS_2 capacitive humidity sensor. *Sensors and Actuators B: Chemical,* 271, 256—263. https://doi.org/10.1016/j.snb.2018.05.084.
6. Lu, Y., Xu, K., Yang, M. Q., Tang, S. Y., Yang, T. Y., Fujita, Y., Takei, K. (2021). Highly stable Pd/HNb_3O_8-based flexible humidity sensor for perdurable wireless wearable applications. *Nanoscale Horiz*, 6, 260—270. https://doi.org/10.1039/D0NH00594K.
7. Karrevula, V. R., Prasad, A. K., Mishra, V., Tripurasundari, S. (2022). Effect of pre-adsorbed moisture and humidity on I—V characteristics of Si PIN diode. *Nuclear Instruments and Methods in Physics Research Section A: Accelerators, Spectrometers, Detectors and Associated Equipment*, 1047, 167832. https://doi.org/ 10.1016/j.nima.2022.167832.
8. Zhao, X., Chen, X., Liu, F., Ding, X., Yu, X., Tang, K., Li, G. (2022). An ultrafast QCM humidity sensor for respiratory monitoring outside a mask. *Sensors and Actuators B: Chemical*, 371, 132396. https://doi.org/10.1016/j.snb.2022.132396.
9. Liu, Y., Gong, H., Lu, X., Ni, K., Zhao, C., Shen, C. (2023). Optical fiber humidity sensor based on vernier effect of Fabry-Perot interferometers with microsphere. *Optical Fiber Technology*, 76, 103222. https://doi.org/10.1016/j.yofte.2023.103222.
10. Shin, Jongmin, Hong, Y., Wu, M., Bae, J. H., Kwon, H. I., Park, B. G., Lee, J. H. (2018). An accurate and stable humidity sensing characteristic of Si FET-type humidity sensor with MoS2 as a sensing layer by pulse measurement. *Sensors and Actuators B: Chemical*, 258, 574—579. https://doi.org/10.1016/j.snb.2017.11.132.
11. Li, X., Tan, Q., Qin, L., Zhang, L., Liang, X., Yan, X. (2022). A high-sensitivity MoS2/graphene oxide nanocomposite humidity sensor based on surface acoustic wave. *Sensors and Actuators A: Physical*, 341, 113573. https://doi.org/10.1016/j.sna.2022.113573.
12. Dusheiko, M. G., Koval, V. M., Obukhova, T. Y. (2022). Silicon nanowire arrays synthesized using the modified MACE process: Integration into chemical sensors and solar cells. *Semiconductor Physics, Quantum Electronics* & *Optoelectronics*, 25, 1, 058—067. https://doi.org/10.15407.SPQEO25.01.058
13. Hou, H., Shao, G., Yang, W., Wong, W. Y. (2020). One-dimensional mesoporous inorganic nanostructures and their applications in energy, sensor, catalysis and adsorption. *Progress in Materials Scienc.,* 113, 100671. https://doi.org/10.1016/j.pmatsci.2020.1006.
14. Hou, H., Shang, M., Wang, L., Li, W., Tang, B., Yang, W. (2015). Efficient photocatalytic activities of TiO_2 hollow fibers with mixed phases and mesoporous walls. *Sci. Rep.*, 5, 15228. https://doi.org/ 10.1038/srep15228.
15. Ren, X., Hou, H., Liu, Z., Gao, F., Zheng, J., Wang, L., Wu, T. (2016). Shape-enhanced photocatalytic activities of thoroughly mesoporous ZnO nanofibers. *Small,* 12, 4007—4017. https://doi.org/10.1002/smll.201600991.
16. Hou, H., Shang, M., Gao, F., Wang, L., Liu, Q., Zheng, J., Yang, W. (2016). Highly efficient photocatalytic hydrogen evolution in ternary hybrid TiO_2/CuO/Cu thoroughly mesoporous nanofibers. *ACS Appl Mater Interfaces*, 8, 20128—20137. https://doi.org/10.1021/acsami.6b06644.
17. Naidonov, A., Koval, V., Barbash, V., Dusheiko, M., Yashchenko, O., Yakymenko, O. (2022). Nanocellulose-Based Biodegradable Bend Sensors. *IEEE 41st International Conference on Electronics and Nanotechnology: "ELNANO", (10—14 October 2022, Kyiv)*, 292—297. https://doi.org/10.1109/ELNANO54667.2022.9927070.

18. Shang, M., Hou, H., Gao, F., Wang, L., Yang, W. (2017). Mesoporous Ag@TiO_2 nanofibers and their photocatalytic activity for hydrogen evolution. *RSC Adv,* 7, 30051—30059. https://doi.org/10.1039/C7RA03177G.
19. Hou, H., Gao, F., Wang, L., Shang, M., Yang, Z., Zheng, J., Yang, W. (2016). Superior thoroughly mesoporous ternary hybrid photocatalysts of TiO_2/WO_3/g-C_3N_4 nanofibers for visible-light-driven hydrogen evolution. *J. Mater. Chem. A*, 4, 6276—6281. https://doi.org/10.1039/C6TA02307J.
20. Linevych, Y., Koval, V., Dusheiko, M., Yakymenko, Y., Lakyda, M., Barbash, V. (2022). Silicon Diode Structures Based on Nanowires for Temperature Sensing Applicatio. *IEEE 42th International Conference on Electronics and Nanotechnology: "ELNANO", (10—14 October 2022, Kyiv),* 190—195. https://doi.org/10.1109/ELNANO54667.2022.9927122
21. Ahmed, N., Bhargav, P. B., Rayerfrancis, A., Chandra, B., Ramasamy, P. (2018). Study the effect of plasma power density and gold catalyst thickness on Silicon Nanowires growth by Plasma Enhanced Chemical Vapour Deposition. *Materials Letters*, 219, 127—130. https://doi.org/10.1016/j.matlet.2018.02.086.
22. Deepu, B. R., Anil, S. M., Savitha, P., Basavaraju, Y. B. (2020). Advanced VLS growth of gold encrusted silicon nanowires Mediated by porous Aluminium Oxide template. *Vacuum*, 185, 109991. https://doi.org/10.1016/j.vacuum.2020.109991.
23. Xi, Y., Zhang, W., Fan, Z., Ma, Q., Wang, S., Ma, D., Zhang, Y. (2018). A facile synthesis of silicon nanowires/micropillars structure using lithography and metal-assisted chemical etching method. *Journal of Solid State Chemistry*, 258, 181—190. https://doi.org/10.1016/j.jssc.2017.07.034.
24. Koval, V., Yakymenko, Y., Ivashchuk, A., Dusheyko, M., Masalskyi, O., Koliada, M., Kulish, D. (2019). Metal-Assisted Chemical Etching of Silicon for Photovoltaic Application. *IEEE 39th International Conference on Electronics and Nanotechnology: "ELNANO", (16—18 April 2022, Kyiv)*, 282—287. https://doi.org/10.1109/ELNANO.2019.8783506
25. Chen, Xuejiao, Zhang, Jian, Wang, Zhiliang, Yan, Qiang, Hui, Shichao. (2011). Humidity sensing behavior of silicon nanowires with hexamethyldisilazane modification. *Sensors and Actuators B: Chemical,* 156.2, 631—636. https://doi.org/10.1016/j.snb.2011.02.009
26. Chen, X., Zhang, J., Wang, Z., Yan, Q., Hui, S. (2008). Investigation of capacitive humidity sensing behavior of silicon nanowires. *Physica E: Low-dimensional Systems and Nanostructures*, 41.4, 600—604. https://doi.org/10.1016/j.physe.2008.10.016.
27. Barillaro, G., Diligenti, A., Strambini, L. M., Comini, E., Faglia, G. (2008). NO_2 adsorption effects on p^+-n silicon junctions surrounded by a porous layer. *Sensors and Actuators B: Chemical*, 134(2), 922—927. https://doi.org/10.1016/j.snb.2008.06.048.
28. Tao, B., Zhang, J., Miao, F., Li, H., Wan, L., Wang, Y. (2008). Capacitive humidity sensors based on Ni/SiNWs nanocomposites. *Sensors and Actuators B: Chemical,* 136.1, 144—150. https://doi.org/10.1016/j.snb.2008.10.039.
29. Hsueh, H. T., Hsueh, T. J., Chang, S. J., Hung, F. Y., Tsai, T. Y., Weng, W. Y., Dai, B. T. (2011). CuO nanowire-based humidity sensors prepared on glass substrate. *Sensors and Actuators B: Chemical,* 156.2, 906—911. https://doi.org/10.1016/j.snb.2011.03.004.

Received 13.04.2023
Revised 11.10.2023
Accepted 19.10.2023

Я.О. Лiневич [1] (https://orcid.org/0000-0002-8399-034),
В.М. Коваль [1] (https://orcid.org/ 0000-0002-3898-9163),
М.Г. Душейко [1] (https://orcid.org/ 0000-0003-3476-4220),
М.О. Лакида [2] (https://orcid.org/0000-00019973-9849)

[1] Національний технічний університет України «Київський політехнічний інститут імені Ігоря Сікорського»,
просп. Перемоги, 37, Київ, 03056, Україна,
+380 44 204 9074, fel@kpi.ua
[2] Національний університет біоресурсів і природокористування України,
вул. Героїв Оборони, 15, Київ, 03041, Україна,
+380 44 527 8205, rectorat@nubip.edu.ua

ДІОДНІ СЕНСОРИ ВОЛОГОСТІ НА ОСНОВІ КРЕМНІЄВИХ 1*D* НАНОРОЗМІРНИХ СТРУКТУР

Вступ. Вимірювання вологості необхідне в мікроелектронній, аерокосмічній, біомедичній та харчовій промисловості, у побуті для клімат-контролю. Наразі як сенсори вологості використовують різні види приладів: ємнісні, резистивні, діодні, гравіметричні та оптичні структури, а також польові транзистори і прилади на поверхневих акустичних хвилях.

Проблематика. На сьогодні є потреба у розробці інтегрально сумісних сенсорів вологи, які мають високу чутливість і низьку вартість. Для цього успішно використано кремнієві нанонитки у сенсорах вологості резистивного та ємнісного типу, проте бракує досліджень щодо впливу нанониток на вологочутливі характеристики сенсорів діодного типу.

Мета. Розробка і дослідження діодних сенсорів вологості на основі кремнієвих нанониток та встановлення впливу технологічних параметрів синтезу та/або структурних особливостей нанониток на робочі характеристики сенсорів вологи.

Матеріали й методи. Процес синтезу сенсорів вологості має кілька етапів: хімічне очищення кремнієвих пластин, синтез кремнієвих нанониток за допомогою стандартного або модифікованого металостимульованого хімічного травлення, дифузія фосфору для створення *p-n*-переходу, фронтальна і тильна металізація. Поверхневу морфологію наноструктур вивчали методом скануючої електронної мікроскопії, дослідження вологочутливих характеристик здійснювали за допомогою сольових гігростатів.

Результати. Показано, що додавання одновимірних кремнієвих наноструктур до складу діодного сенсора вологи значно покращило його робочі характеристики: коефіцієнт випрямлення зріс з 161 до 1807, відгук — з 4,5 до 25, чутливість — з 1,6 до 4,02 $(\%RH)^{-1}$, тоді як час відгуку та час відновлення зменшилися з 85/90 до 25/30 с, величина гістерезису — з 75 до 16 %, девіація сигналу після циклювання — з 15 до 3 %, флуктуація сигналу під час неперервної роботи сенсора — з 17 до 15 %.

Висновки. Використання простоїв та дешевої технології синтезу нанодротів є ефективним для виробництва сенсорів вологи.

Ключові слова: металостимульоване хімічне травлення, кремнієві нанонитки, 1*D* наноструктури, кремнієвий діод, сенсори вологи.